Platinum(II) and Palladium(II) Dibenzo[*a*,*e*]cyclooctatetraene (DBCOT) Oxo and Halide Complexes: Comparison to 1,5-COD Analogues

Anupam Singh and Paul R. Sharp*

125 Chemistry, University of Missouri, Columbia, Missouri 65211

Received August 17, 2005

The dialkene complexes L_2MCl_2 (M = Pt, Pd, L_2 = dibenzo[*a*,*e*]cyclooctatetraene (DBCOT)) were prepared by treatment of MCl_4^{2-} salts with L_2. Comparison of the solid-state structures with those of the analogous 1,5-cyclooctadiene (COD) complexes shows strong congruence of the structures. Competition experiments between DBCOT and COD show that COD bonds more strongly to the Pt(II) center. In contrast, Ir(I) bonds slightly better to DBCOT. Reaction of $PtCl_2$(DBCOT) with NaI gives PtI_2(DBCOT), which reacts with PhMgBr to give $PtPh_2$(DBCOT). ^{195}Pt NMR data indicate a less electron-rich Pt center in the DBCOT complexes as compared to the analogous COD complexes. Treatment of $PtCl_2$(DBCOT) with $[(Ph_3PAu)_3(\mu^3\text{-}O)](BF_4)$ yields trimeric $[Pt(\mu^3\text{-}O)(DBCOT)(AuPPh_3)]_3(BF_4)_3$, which contains a six-membered Pt_3O_3 ring in a twist-boat configuration. Au−Au and Au−Pt interactions may help stabilize the solid-state structure, but NMR and mass spectral data indicate a dynamic structure in solution and the likely presence of other oligomers.

Introduction

The chelating diene ligand 1,5-cyclooctadiene (COD) has been prominent in transition metal chemistry.[1] This is especially true for the late transition metals where COD has provided a variety of stable but labile complexes many of which are starting materials for further chemistry.[2] Our group has used COD as a supporting ligand for Pt, Rh, and Ir oxo chemistry.[3] The COD Pt oxo chemistry has proved to be particularly interesting, producing the oxo complex $[Pt_2(\mu\text{-}O)Cl(COD)_2]_2$ (**1**)[4] that oxidizes alkenes.[5] Remarkably, the COD ligand is not itself oxidized in this system but seems to provide unique properties.

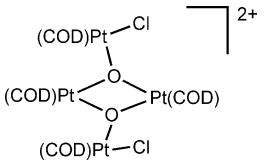

1

In our efforts to understand and expand this chemistry we have attempted to substitute COD with other ligands and to prepare a Pd analogue of **1**. Pd and Pt oxo complexes[6,7] with diimine ligands have been successfully prepared, but, like our previously prepared Pt oxo complexes with phosphine ligands,[8−10] none of these new complexes show the alkene oxidation reactivity of **1**. Attempts to prepare Pt oxo complexes with NBD, a cyclic diene that has yielded many COD analogues, were not successful nor were attempts to prepare NBD or COD Pd oxo complexes. Free NBD and COD were observed in the Pd reaction mixtures, suggesting that a more strongly bonding analogue of COD is needed.

In searching for a strongly bonding chelating diene ligand, we came across dibenzo[*a*,*e*]cyclooctatetraene (DBCOT). DBCOT is believed to bond more strongly to metal centers than COD.[11] Strong bonding and its resistance to hydrogenation has led to the use of DBCOT as a poison for homogeneous catalysts.[12] A recent report of an improved DBCOT synthesis[13] and a facile preparation of substituted DBCOTs[14] makes this dialkene ligand particularly attractive for investigation. Here we report the synthesis, characterization, and structures of Pt(II) and Pd(II) complexes with the DBCOT ligand and compare the stability and reactivity of $PtCl_2$(DBCOT) with $PtCl_2$(COD).

Results

Yellow $PtCl_2$(DBCOT) (**2**) and orange $PdCl_2$(DBCOT) (**3**)[15] are readily prepared in good yields from K_2PtCl_4 and Na_2PdCl_4 by procedures similar to those reported for the COD analogues.[16,17] Both complexes are somewhat more soluble than

* To whom correspondence should be addressed. E-mail: SharpP@missouri.edu.

(1) *Comprehensive Organometallic Chemistry II*; Pergamon: Oxford, 1995.

(2) See the subject indexes of *Inorg. Synth.* volumes 25 and 28 under 1,5-cyclooctadiene.

(3) Sharp, P. R. *J. Chem. Soc., Dalton Trans.* **2000**, 2647−2657.

(4) Shan, H.; James, A. J.; Sharp, P. R. *Inorg. Chem.* **1998**, *37*, 5727−5732.

(5) Szuromi, E.; Hui, S.; Sharp, P. R. *J. Am. Chem. Soc.* **2003**, *124*, 10522−10523.

(6) Singh, A.; Sharp, P. R. *Dalton Trans.* **2005**, 2080−2081.

(7) Anandhi, U.; McGee, C.; Sharp, P. R. Unpublished results.

(8) Li, J. J.; Sharp, P. R. *Inorg. Chem.* **1994**, *33*, 183−184.

(9) Li, J. J.; Li, W.; Sharp, P. R. *Inorg. Chem.* **1996**, *35*, 604−613.

(10) Li, J. J.; Li, W.; James, A. J.; Holbert, T.; Sharp, T. P.; Sharp, P. R. *Inorg. Chem.* **1999**, *38*, 1563−1572.

(11) Anton, D. R.; Crabtree, R. H. *Organometallics* **1983**, *2*, 621−627.

(12) Anton, D. R.; Crabtree, R. H. *Organometallics* **1983**, *2*, 855−859.

(13) Chaffins, S.; Brettreich, M.; Wudl, F. *Synthesis* **2002**, 1191−1194.

(14) Läng, F.; Breher, F.; Stein, D.; Grützmacher, H. *Organometallics* **2005**, *24*, 2997−3007.

(15) Avram, M.; Dinu, D.; Mateescu, G.; Nenitzescu, C. D. *Chem. Ber.* **1960**, *93*, 1789−1794.

10.1021/om050713w CCC: $33.50
Publication on Web 12/20/2005

their COD analogues, dissolving readily in halogenated solvents but less readily in aromatic solvents.

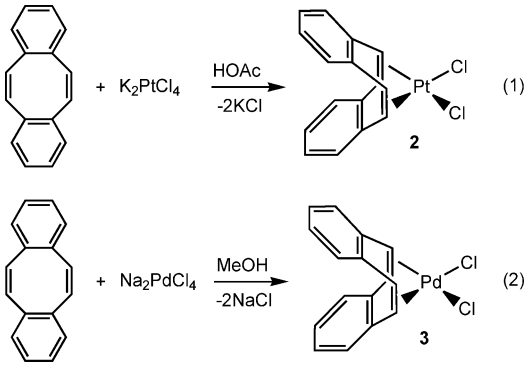

The ^{1}H NMR spectrum of **2** shows the resonances of the aromatic protons of the DBCOT ligand as a singlet at 7.17 ppm, indicating accidental coincidence of the two aromatic proton signals. The olefinic protons appear as a sharp singlet at 6.56 ppm with Pt satellites (J_{Pt-H} = 59.3 Hz). The ^{195}Pt NMR spectrum of **2** shows a quintet at −2974 ppm (J_{Pt-H} = 59.3 Hz), confirming the coupling between the olefinic protons and the Pt center. The ^{1}H NMR spectrum of **3** shows the resonances for the aromatic protons as a symmetric pattern at 7.28−7.13 ppm, similar to that seen in the free ligand. The olefinic protons are found as a singlet at 6.95 ppm.

To investigate the stability of DBCOT complex **2** relative to the COD analogue, an equimolar mixture of **2** and COD in methylene chloride in a flame-sealed NMR tube was monitored by ^{1}H NMR spectroscopy. There was no change in the mixture after 14 h at room temperature. Heating the mixture at 60−90 °C for 2 days gave complete conversion to $PtCl_2$(COD) and free DBCOT with no detectable concentrations of **2** or COD. Addition of 20 equiv of DBCOT to a fresh mixture dramatically slowed the reaction such that after 10 days at 90 °C the reaction was 50% complete and still slowly progressing. A mixture of $PtCl_2$(COD) and 20 equiv of DBCOT showed no change after 7 days at 90 °C. In none of these reactions were there any visual or spectroscopic signs of decomposition. Assuming a detection limit of 1%, this places a lower limit of ca. 10^5 on the equilibrium constant for the reaction shown in eq 3.

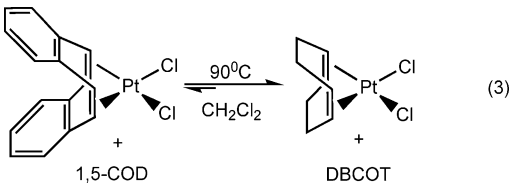

Despite the weaker bonding of the DBCOT ligand, **2** still undergoes chemistry similar to $PtCl_2$(COD).[18] Dichloride **2** is readily converted to the diiodide PtI_2(DBCOT) (**4**) in 98% yield by addition of NaI to a suspension of **2** in acetone. The ^{1}H NMR spectrum of **4** is similar to that for **2** (including the accidental coincidence of the two aromatic signals) except that the signals are at higher frequency than those for **2**. The ^{195}Pt NMR spectrum of **4**, like **2**, shows a quintet (J_{PtH} = 59.0 Hz) at −2439.7 ppm but to higher frequency than that of **2**.

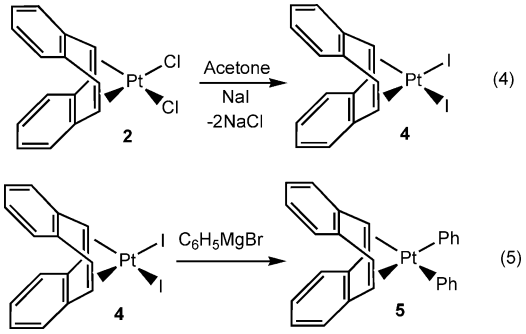

The diphenyl complex $PtPh_2$(DBCOT) (**5**) is obtained from the reaction of **4** with phenylmagnesium bromide.[19] The ^{1}H NMR spectrum of complex **5** shows aromatic resonances at 7.63−7.04 and 6.90−6.77 ppm with the olefinic protons at 6.14 ppm with Pt satellites (J_{Pt-H} = 33.0 Hz). The ^{195}Pt NMR resonance for **5** is at −3260.2 ppm. This is at lower frequency than those for **2** and **4**, but the smaller Pt−H coupling is not resolved and the signal is a singlet.

Yellow **6** is isolated from the oxo−chloro exchange reaction[3] between gold oxo complex [(AuPPh$_3$)$_3$(μ^3-O)](BF$_4$) and $PtCl_2$(DBCOT) in an equimolar ratio in THF (eq 6). Further addition of $PtCl_2$(DBCOT), which in the case of COD gave **1**,[4] does not give any new products. The solid-state structure of **6** was determined by an X-ray crystal structure determination (see below and Figure 3). In contrast to the analogous COD reaction, which yields the dimer [Pt(μ^3-O)(COD)(AuPPh$_3$)]$_2^{2+}$,[4] **6** is the trimer [Pt(μ^3-O)(DBCOT)(AuPPh$_3$)]$_3^{3+}$. However, spectroscopic data suggest the presence of other species such as a dimer in solutions of **6** probably in equilibrium with the isolated trimer (eq 6).

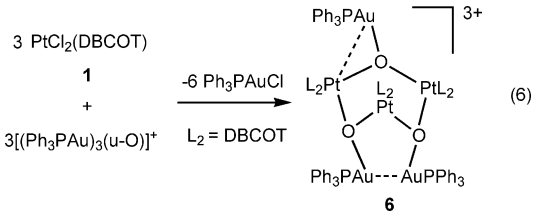

The ^{31}P NMR spectrum of **6** at room temperature shows a singlet at 27.5 ppm. At −70 °C the peak slightly broadens but does not resolve into the 1:2 pattern expected from the solid-state structure. In contrast the ^{1}H NMR spectrum of **6** is complex and highly temperature and solvent dependent. At ambient probe temperature the spectrum in $CDCl_3$ shows two sets of multiplets at 7.4 and 7.1 ppm and two broad overlapping singlets in a ca. 3:1 ratio at 6.75 and 6.68 ppm. Coupling to Pt characteristic of the olefinic protons is not discernible. In CD_2Cl_2 three sets of multiplets at 7.45, 7.1, and 6.8 ppm are observed along with two singlets at 6.70 and 6.28 ppm in a 2:1 ratio. The singlet at 6.28 ppm is broad. Again, coupling to Pt is not visible. Cooling the CD_2Cl_2 sample results in a broadening and collapse of the signals such that at −70 °C there is an irregular broad peak from 6.1 to 7.6 ppm under a somewhat sharper multiplet at 7.4 ppm. We attribute this behavior partly to exchange of the different Ph_3PAu fragments, but equilibrium

(16) McDermott, J. X.; White, J. F.; Whitesides, G. M. *J. Am. Chem. Soc.* **1976**, *98*, 6521−6528.
(17) Drew, D.; Doyle, J. R. *Inorg. Synth.* **1990**, *28*, 346−349.
(18) Clark, H. C.; Manzer, L. E. *J. Organomet. Chem.* **1973**, *59*, 411−428.
(19) For a new preparation of $PtPh_2$(COD) directly from $PtCl_2$(COD) see: Shekhar, S.; Hartwig, J. F. *J.* Am. Chem. Soc. **2004**, *126*, 13016−13027.

Table 1. Crystallographic and Data Collection Parameters for 1−4[a]

	1	2	3	4
formula	$C_{16}H_{12}Cl_2Pt\cdot 2CH_2Cl_2$	$C_{16}H_{12}Cl_2Pd\cdot 2CH_2Cl_2$	$C_{16}H_{12}I_2Pt\cdot 0.5CH_2Cl_2$	$[C_{102}H_{81}Au_3O_3P_3Pt_3][BF_4]_3\cdot 10CHCl_3$
fw	640.1	520.84	695.61	4077.86
cryst syst	triclinic	triclinic	orthorhombic	monoclinic
space group	$P\bar{1}$	$P\bar{1}$	*Pbcn*	$P2_1/c$
a, Å	8.7025(15)	8.6556(5)	13.1530(12)	14.5038(9)
b, Å	11.418(2)	11.4257(6)	16.0334(14)	36.472(2)
c, Å	11.949(2)	11.9665(7)	32.836(3)	26.1887(16)
α, deg	64.326(3)	63.9610(10)	90	90
β, deg	88.254(3)	87.5790(10)	90	97.8320(10)
γ, deg	78.493(3)	78.2270(10)	90	90
V, Å^3	1046.4(3)	1039.44(10)	6924.7(11)	13724.0(15)
Z	2	2	16	4
d_{calc}, g/cm^3	2.03	1.76	2.67	1.974
μ, mm^{-1}	7.47	1.66	11.815	6.92
R1,[b] wR2[c]	0.0376, 0.0984	0.0326, 0.0791	0.0464, 0.0969	0.0827, 0.1808

[a] $\lambda = 0.71070$ Å (Mo), $T = -100$ °C. [b] $R1 = (\sum||F_o| - |F_c||)/\sum|F_o|$. [c] $wR2 = [(\sum w(F_o^2 - F_c^2)^2)/\sum w(F_c^2)^2]^{1/2}$.

between a dimer and trimer form of **6** (eq 7) probably also contributes, as suggested by the ESI mass spectrum of an acetonitrile solution of **6**.

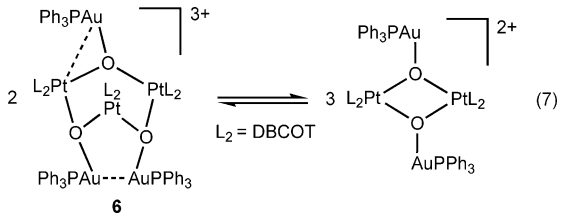

(7)

The first three most intense peaks in the mass spectrum (ESI/APC-direct infusion) of **6** are assigned to $[Ph_3PAuNCMe]^+$, $[(Ph_3P)_2Au]^+$, and $[(Ph_3PAu)_2Cl]^+$. The next most intense peak at *m*/*z* 1289 is attributed to the dimer fragment $[Pt_2(O)_2(DBCOT)_2(AuPPh_3)]^+$ produced by loss of Ph_3PAu^+ from the dimer $[Pt(\mu^3\text{-}O)(DBCOT)(AuPPh_3)]_2^{2+}$. The isotope pattern match for all of these peaks is excellent. The next most intense peak at *m*/*z* 874 could be due to the trimer $[Pt(\mu^3\text{-}O)(DBCOT)(AuPPh_3)]_3^{3+}$ or the dimer $[Pt(\mu^3\text{-}O)(DBCOT)(AuPPh_3)]_2^{2+}$. However, the peak pattern does not match either species or a combination of the two, making a positive assignment out of reach.

Structures. A summary of crystal data and data collection and processing is given in Table 1. Selected distances and angles are given in Tables 2 and 3. Drawings of the solid-state structures of **2** and **6** are given in Figures 1 and 2. Those for **3** and **4** are provided in the Supporting Information.

The structures of **2** and $PtCl_2(COD)$[20] are highly congruent, as shown by a comparison of the averaged metrical parameters in Table 4. The average Pt−C, Pt−Cl, and coordinated C═C double bond lengths are identical within experimental error, as are the angles around the Pt atoms. The one feature that is different is the angle of the coordinated olefinic unit to the Pt coordination plane. The double bonds are essentially perpendicular to the plane (89.9° and 89.2°) in **2** but somewhat canted in $PtCl_2(COD)$ (83.4° and 83.3°).

Crystals of $PdCl_2(DBCOT)$ (**3**) are isomorphous with those of **2**. The compounds are isostructural but with the expectedly longer metal−carbon distances for **3** (Table 2). As with **2** a comparison with the COD analogue[21−23] reveals no differences in the essential features of the structure with the exception of the angle of the coordinated olefinic unit to the Pd coordination plane. This is again at nearly 90° for **3** (89.8 and 89.2) but canted in $PdCl_2(COD)$ (83.6 and 84.9, 83.2 and 83.3).

Table 2. Selected Distances and Angles for 2−4

	$PtCl_2(DBCOT)$ (**2**)	$PdCl_2(DBCOT)$ (**3**)	$PtI_2(DBCOT)$ (**4**)	$PtI_2(DBCOT)$ (**4**)[a]
M−X1	2.2999(16)	2.2914(8)	2.6121(7)	2.6119(9)
M−X2	2.3110(16)	2.3000(7)	2.6007(8)	2.5968(9)
M−C1	2.181(6)	2.206(3)	2.204(9)	2.193(10)
M−C2	2.162(6)	2.202(3)	2.197(10)	2.211(10)
M−C9	2.161(6)	2.207(3)	2.209(10)	2.208(10)
M−C10	2.173(6)	2.207(3)	2.200(9)	2.204(10)
M−C (av)	2.169(10)	2.206(2)	2.203(6)	
C1−C2	1.388(9)	1.385(4)	1.391(14)	1.382(15)
C2−C3	1.486(9)	1.486(4)	1.474(13)	1.499(14)
C3−C8	1.405(8)	1.397(4)	1.387(15)	1.398(15)
C8−C9	1.487(8)	1.485(4)	1.472(14)	1.478(16)
C9−C10	1.390(8)	1.380(4)	1.433(15)	1.440(14)
C10−C11	1.497(8)	1.490(4)	1.497(14)	1.480(13)
C11−C16	1.383(9)	1.395(4)	1.385(14)	1.390(14)
C1−C16	1.491(9)	1.487(4)	1.490(14)	1.493(14)
X1−M−X2	89.55(6)	90.10(3)	91.43(3)	90.18(3)
||−M−||[b]	88.1	87.2	86.7	86.6
C2−C1−M	70.6(3)	71.52(17)	71.3(5)	72.5(6)
C1−C2−M	72.1(4)	71.85(17)	71.9(6)	71.0(6)
C10−C9−M	71.8(3)	71.80(17)	70.7(6)	70.8(6)
C9−C10−M	70.8(3)	71.78(17)	71.4(5)	71.1(5)
C16−C1−M	107.5(4)	107.5(2)	108.8(7)	107.7(7)
C3−C2−M	108.5(4)	107.21(18)	107.7(7)	109.4(7)
C11−C10−M	108.2(4)	107.81(19)	108.4(6)	108.6(6)
C8−C9−M	108.4(4)	107.15(19)	107.5(7)	108.8(6)
C2−C1−C16	123.7(6)	124.4(3)	125.2(9)	123.7(9)
C1−C2−C3	124.5(6)	124.8(3)	124.2(8)	123.2(9)
C10−C9−C8	123.1(5)	123.8(3)	123.3(9)	123.7(9)
C9−C10−C11	123.8(6)	124.1(3)	123.7(9)	122.7(9)

[a] Molecule 2 of 2. [b] || represents C1−C2 and C9−C10 centroids.

Crystals of $PtI_2(DBCOT)$ (**4**) are not isomorphous with those of **2** and **3** and contain two independent molecules in the asymmetric unit. However, **4** is isostructural with **2** and **3** but with the expectedly longer metal−iodine distances for **4** (Table 2). All other features match those of **2** and **3**.

The core structure of the cationic portion of oxo complex **6** is shown in Figure 2 (a complete drawing is available in the Supporting Information) and is a trimer of $[(DBCOT)Pt-O-AuPPh_3]^+$ units linked through Pt−O bonds. The result is a six-membered Pt−O ring in a distorted twist-boat conformation with Pt1 and O2 in the unique "up" positions and Au2 occupying a

(20) Syed, A.; Stevens, E. D.; Cruz, S. G. *Inorg. Chem.* **1984**, *23*, 3673−3674.

(21) Rettig, M. F.; Wing, R. M.; Wiger, G. R. *J. Am. Chem. Soc.* **1981**, *103*, 2980−2986.

(22) T. Kumar, R.; Maverick, A. W.; Fronczek, F. R.; Doyle, J. R.; Baenziger, N. C.; Howells, M. A. M. *Acta Crystallogr., C* **1993**, *C49*, 1766−1767.

(23) Benchekroun, L.; Herpin, P.; Julia, M.; Saussine, L. *J. Organomet. Chem.* **1977**, *128*, 275−290.

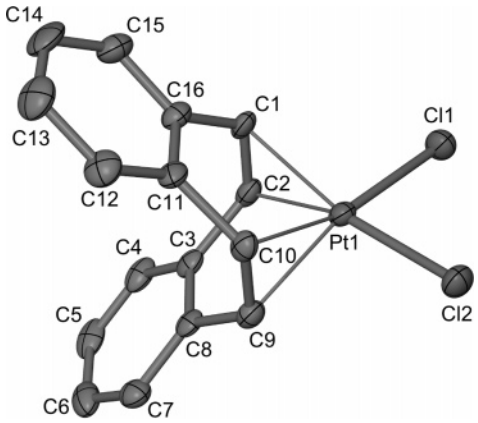

Figure 1. Plot of the solid-state structure of $PtCl_2$(DBCOT) (50% probability ellipsoids, hydrogen atoms omitted).

Table 3. Selected Distances and Angles for 6

Au1−Pt1	3.0057(12)	Au3−O3	2.084(14)
Au2−Pt2	3.1150(12)	Pt1−O1	2.022(15)
Au3−Pt3	3.0556(12)	Pt1−O3	1.975(13)
Au1−Au3	3.1087(12)	Pt2−O1	1.981(15)
Au1−P1	2.213(6)	Pt2−O2	2.028(14)
Au2−P2	2.214(6)	Pt3−O2	1.976(14)
Au3−P3	2.217(6)	Pt3−O3	1.998(14)
Au1−O1	2.075(15)	Pt−O (av)	2.00(2)
Au2−O2	2.076(14)	Pt−C (av)	2.18(2)
O1−Au1−P1	171.8(4)	O3−Pt1−O1	90.4(6)
O2−Au2−P2	173.4(4)	O1−Pt2−O2	95.0(6)
O3−Au3−P3	160.3(4)	O2−Pt3−O3	89.6(5)
O1−Au1−Au3	79.6(4)	O2−Pt2−Au2	41.2(4)
P1−Au1−Au3	103.18(17)	O1−Pt2−Au2	92.0(4)
Pt1−Au1−Au3	73.47(3)	O2−Pt3−Au3	83.4(4)
O1−Au1−Pt1	42.1(4)	O3−Pt3−Au3	42.6(4)
P1−Au1−Pt1	130.91(17)	Pt2−O1−Pt1	122.6(8)
O2−Au2−Pt2	40.1(4)	Pt3−O2−Pt2	134.5(7)
P2−Au2−Pt2	137.28(15)	Pt1−O3−Pt3	112.1(6)
O3−Au3−Pt3	40.5(4)	Pt2−O1−Au1	118.1(7)
P3−Au3−Pt3	125.26(17)	Pt1−O1−Au1	94.4(6)
O3−Au3−Au1	75.7(4)	Pt3−O2−Au2	116.6(7)
P3−Au3−Au1	123.44(17)	Pt2−O2−Au2	98.7(6)
Pt3−Au3−Au1	107.88(3)	Pt1−O3−Au3	128.6(7)
O1−Pt1−Au1	43.5(4)	Pt3−O3−Au3	96.9(6)
O3−Pt1−Au1	79.7(4)		

flagpole position on O2. Au1 and Au3 occupy adjacent "axial" positions, allowing them to participate in aurophilic[24] interactions. There are also short Pt−Au distances (Pt1−Au1, Pt3−Au3, Pt2−Au2), indicating related closed shell Pt−Au interactions.[25−29] Despite the presence of two different types of Pt and O centers, the Pt−O distances (1.975(13)−2.028(14) Å) are identical within experimental error, as are the Au−O distances (2.075(15)−2.084(14) Å). However, the O−Pt−O angles do differ, with the unique O1−Pt2−O2 angle significantly greater (95.6(6)°) than the corresponding angles of Pt1 (90.4(6)°) and Pt3 (89.6(5)°). The angles around the oxo groups vary considerably. Among the Pt−O−Pt angles, that for unique O2 is largest at 134.5(7)° followed by O1 (122.6(8)°) and O3 (112.1(6)°). The Pt−O−Au angles occur in sets of one large and one small for each oxo ligand (e.g., 118.1(7)° and 94.4(6)° for O1). This is due to the Au−Pt interactions, which draw the

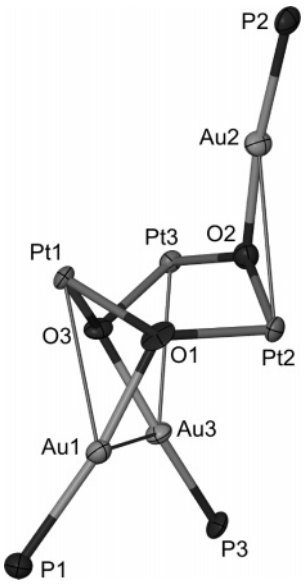

Figure 2. Drawing of the core structure of the cationic portion of oxo complex **6** (50% probability ellipsoids, hydrogen and carbon atoms omitted).

Table 4. Comparison of the Average Metrical Parameters for $PtCl_2$(DBCOT) (2) and $PtCl_2$(COD)

	$PtCl_2$(DBCOT) (**2**)	$PtCl_2$(COD)
Pt−C1	2.305(8)	2.312(4)
Pt−C	2.169(10)	2.170(11)
C═C	1.389(9)	1.381(8)
Cl−Pt−Cl	89.55(6)	89.78(5)
||−Pt−||[a]	88.1(2)	87.3(2)
C−C═C	123.8(6)	125.0(6)

[a] || represents C1−C2 and C9−C10 centroids.

Au atoms closer to one of the two Pt atoms in the oxygen-centered Pt_2Au triangles.

The trimeric structure of **6** with Pt−Au and Au−Au interactions is in contrast to the analogous COD product, which is the dimer $[Pt(\mu^3\text{-}O)(COD)(AuPPh_3)]_2(BF_4)_2$.[4] There are no Au−Au or Pt−Au interactions in the dimer, and the $Pt_2O_2Au_2$ core is nearly planar. As a result of the smaller ring size for the COD complex (**4** vs **6**), the internal angles are much smaller. For example, the O−Pt−O angle is 79.5(3)° in the dimer as compared to the 112−135° range observed for **6**. Despite these differences, the average Pt−O distances are the same in both complexes, at 2.012(7) Å for the COD complex and 2.00(2) Å for **6**. On the other hand, the Au−O distances are somewhat shorter in the COD complex (2.026(6) Å) than in **6** (2.078(5) Å). The longer distances in **6** may result from the distortions caused by the Au−Au and Au−Pt interactions.

Discussion

The weaker bonding of the DBCOT ligand in $PtCl_2$(DBCOT) in comparison to $PtCl_2$(COD) is in sharp contrast to the reported observations on related Ir(I) complexes.[11] $[Ir(\mu\text{-}Cl)(DBCOT)]_2$ was readily obtained from the room-temperature reaction of $[Ir(\mu\text{-}Cl)(COD)]_2$ with 1 equiv of DBCOT, implying that the DBCOT complex is more stable than the COD complex. However, $[Ir(\mu\text{-}Cl)(DBCOT)]_2$ is much less soluble than $[Ir(\mu\text{-}Cl)(COD)]_2$ and precipitates from the reaction mixture. Precipitation could shift an unfavorable equilibrium such that $[Ir(\mu\text{-}Cl)(DBCOT)]_2$ could be isolated even if it is less stable than the COD complex. To investigate this possibility, we examined the reaction of $[Ir(\mu\text{-}Cl)(COD)]_2$ with DBCOT in

(24) Schmidbaur, H. *Gold Bull.* **2000**, *33*, 3−10.
(25) Pyykkö, P. *Chem. Rev.* **1997**, *97*, 597−636.
(26) Jeffery, J. C.; Jelliss, P. A.; Stone, F. G. A. *Inorg. Chem.* **1993**, *32*, 3943−3947.
(27) Hadj-Bagheri, N.; Puddephatt, R. J. *Inorg. Chim. Acta* **1993**, *213*, 29.
(28) Tanase, T.; Toda, H.; Yamamoto, Y. *Inorg. Chem.* **1997**, *36*, 1571.
(29) Yip, H. K.; Lin, H. M.; Wang, Y.; Che, C. M. *J. Chem. Soc., Dalton Trans.* **1993**, 2939−2944.

various ratios and at two concentrations. The reactions were monitored by ^{1}H NMR spectroscopy. In the more concentrated samples precipitation occurred 3−24 h after mixing. There was no change in the mixture up to precipitate formation. In the more dilute sample no precipitation was observed up to 1 week and the ^{1}H NMR spectrum did not change over this time period, suggesting that equilibrium of the complexes with each other in solution is achieved quickly. Free COD and $[Ir(\mu\text{-Cl})(DBCOT)]_2$ were observed along with remaining DBCOT and $[Ir(\mu\text{-Cl})(COD)]_2$. Another COD species with peaks very close to those for $[Ir(\mu\text{-Cl})(COD)]_2$ was also observed. This is assigned to the mixed DBCOT/COD dimer $Ir_2(\mu\text{-Cl})_2(COD)(DBCOT)$. This same complex is formed from a mixture of $[Ir(\mu\text{-Cl})(COD)]_2$ and $[Ir(\mu\text{-Cl})(DBCOT)]_2$. By integration of the peaks for complexed and free ligands an equilibrium constant of 8 ± 1 was obtained for the equilibrium shown in eq 8, where (DBCOT)Ir(I) and (COD)Ir(I) represent the amount of each complexed ligand in both the pure dimers and the mixed dimer. Calculated equilibrium constants for dilute solution (no precipitate) and the more concentrated solutions agree.

$$(COD)Ir(I) + DBCOT \rightleftharpoons (DBCOT)IR(I) + COD \quad (8)$$

Thus, DBCOT appears to bond slightly better to Ir(I) than COD. This difference between Ir(I) and Pt(II) may arise from differences in the relative importance of the donor and acceptor components of the bonding to the olefinic unit. DBCOT is a weaker σ-donor but better π-acceptor than COD[11] and the donor component is likely more important for Pt(II) than for Ir(I). Consistent with weaker σ-donor but better π-acceptor character, IR studies have shown that the DBCOT ligand is substantially more electron-withdrawing than COD.[11]

Weaker bonding of DBCOT to Pt(II) is supported by the ^{195}Pt NMR shifts. The ^{195}Pt NMR signal for $PtCl_2(DBCOT)$ (−2975) is at higher frequency by 362 ppm from that for $PtCl_2(COD)$ (−3337 ppm). A correlation of ^{195}Pt NMR shifts with the strength of alkene bonding has previously been noted for a series of Zeise's salt analogues, with the more stable complexes showing the lowest frequency shifts.[30,31] Similarly, a comparison of the Pt−C coupling constants of $PtCl_2(DBCOT)$ (J_{Pt-C} = 136.3 Hz) and $PtCl_2(COD)$ (J_{Pt-C} = 152.5 Hz) indicates a weaker Pt−C interaction.

Comparison of the structures of $PtCl_2(DBCOT)$ and $PtCl_2(COD)$ does not reveal any significant differences in the structures that would indicate weaker bonding for the DBCOT ligand. The lower stability of $PtCl_2(NBD)$ as compared to $PtCl_2(COD)$ has been attributed to the smaller bite angle of NBD (70.3°),[32] but the essentially identical structures of $PtCl_2(DBCOT)$ and $PtCl_2(COD)$ with bite angles of 88.1° and 87.3° eliminates this possibility, indicating that electronic factors are involved. The lack of structural indicators for weaker bonding is consistent with the structures of σ-donor/π-acceptor complexes, which show that complex geometry is a poor indicator of ligand bond strength.[33,34]

Despite the weaker bonding, our brief investigation of $PtCl_2(DBCOT)$ has revealed chemistry generally analogous to that of $PtCl_2(COD)$. However, the oxo chemistry that interested us most is significantly different. The 1:1 reaction with the gold oxo complex gave instead of the dimer observed with COD, trimer **6**. Solution data including mass spectral results suggest that the DBCOT dimer does exist in solution in equilibrium with the trimer and perhaps other oligomers. This may also be true of the COD complex, though no evidence for this has been detected. Solubility would then determine which oligomer is isolated. This is reminiscent of Pt(II) hydroxo complexes of formula $[Pt(\mu\text{-OH})L_2]_n^{n+}$, which have been isolated as dimers (n = 2), trimers (n = 3), and tetramers (n = 4).[35−40] As the Ph_3PAu^+ fragment is isolobal with the proton,[41] oxo complexes of empirical formula $[L_2Pt(\mu\text{-OAuL})]^+$ are analogues of the hydroxo complexes.

The greater electrophilicity of the Pt center in the $Pt(DBCOT)^{2+}$ unit may be responsible for the isolation of the trimer. The COD dimer does not have metal−metal interactions. In contrast, DBCOT oxo complex **6** has both Pt−Au and Au−Au interactions. These interactions may contribute to the stability of the trimer structure in comparison to the dimer structure. While Au−Pt interactions are still possible in the more rigid dimer structure with its four-membered Pt_2O_2 ring,[3] Au−Au interactions would be difficult to attain with the strong steric interactions that would be present with Ph_3PAu^+ units on the same side of the Pt_2O_2 ring.

A more significant difference between the DBCOT and COD chemistry is the failure of trimer **6** to react further with the gold oxo complex $[(Ph_3PAu)_3(\mu\text{-O})]^+$. The COD dimer yields the all-Pt oxo complex **1** when treated with additional gold oxo complex. Oxo complex **1** is unique in its reactions with alkenes, and we anticipated analogous chemistry with DBCOT. The failure of the DBCOT system to yield an analogue of **1** is unexplained, as is the failure of the NBD ligand system.

Conclusions

Simple DBCOT analogues of Pt and Pd COD complexes are readily prepared using procedures similar to those for the COD complexes. The DBCOT ligand is more electron-withdrawing than the COD ligand and, in contrast to Ir(I), bonds more weakly to Pt(II) than COD.

Experimental Section

General Procedures. DBCOT (dibenzo[*a*,*e*]cyclooctatetraene),[13] $[(LAu)_3(\mu^3\text{-O})]BF_4$ (L = PPh_3),[42] and $[Ir(\mu\text{-Cl})(COD)]_2$[43] were prepared by literature procedures. Phenylmagnesium bromide (3 M in diethyl ether) was purchased from Aldrich. Experiments were performed under a dinitrogen atmosphere in a Vacuum Atmospheres Corporation drybox or on a Schlenk line with dried and degassed solvents stored under dinitrogen over 4 Å molecular sieves or sodium metal. NMR spectra were recorded on a Bruker AMX-

(30) Öhrström, L. *Comments Inorg. Chem.* **1996**, *18*, 305−323.
(31) Erickson, L. E.; Hayes, P.; Hooper, J. J.; Morris, K. F.; Newbrough, S. A.; Van Os, M.; Slangan, P. *Inorg. Chem.* **1997**, *36*, 284−290.
(32) Butikofer, J. L.; Kalberer, E. W.; Schuster, W. C.; Roddick, D. M. *Acta Crystallogr., C* **2004**, *C60*, m353−m354.
(33) Huang, J. K.; Haar, C. M.; Nolan, S. P.; Marshall, W. J.; Moloy, K. G. *J. Am. Chem. Soc.* **1998**, *120*, 7806−7815.
(34) Massera, C.; Frenking, G. *Organometallics* **2003**, *22*, 2758−2765.
(35) Macquet, J.-P.; Cros, S.; Beauchamp, A. L. *J. Inorg. Biochem.* **1985**, *25*, 197.
(36) Rochon, F. D.; Morneau, A.; Melanson, R. *Inorg. Chem.* **1988**, *27*, 10.
(37) Faggiani, R.; Lippert, B.; Lock, C. J. L.; Rosenberg, B. *Inorg. Chem.* **1978**, *17*, 1941−1945.
(38) Faggiani, R.; Lippert, B.; Lock, C. J. L.; Rosenberg, B. *Inorg. Chem.* **1977**, *16*, 1192−1196.
(39) Wimmer, S.; Castan, P.; Wimmer, F. L.; Johnson, N. P. *J. Chem. Soc., Dalton Trans.* **1989**, 403−412.
(40) Gill, D. S.; Rosenberg, B. *J. Am. Chem. Soc.* **1982**, *104*, 4598−4604.
(41) Evans, D. G.; Mingos, D. M. P. *J. Organomet. Chem.* **1982**, *232*, 171−191.
(42) Nesmeyanov, A. N.; Perevalova, E. G.; Struchkov, Y. T.; Antipin, M. Y.; Grandberg, K. I.; Dyadchenko, V. P. *J. Organomet. Chem.* **1980**, *201*, 343−349.
(43) Herde, J. L.; Lambert, J. C.; Senoff, C. V. *Inorg. Synth.* **1974**, *15*, 18−20.

250, -300, or -500 spectrometer at ambient probe temperatures. Shifts are given in ppm with positive values to higher frequency of TMS (^{1}H and ^{13}C), external H_3PO_4 (^{31}P), or external K_2PtCl_4(aq) (^{195}Pt, −1630 ppm). ^{13}C and ^{1}H NMR spectra were recorded in proton-decoupled mode. Desert Analytics performed the microanalyses (inert atmosphere). The presence of solvent of crystallization in the analyzed sample was confirmed by NMR spectroscopy. The Chemistry Mass Spectrometry Facility at The Ohio State University collected the mass spectral data for the organic products.

Dichloro(dibenzo[*a,e*]cyclooctatetraene)platinum(II), $PtCl_2$(DBCOT) (2). K_2PtCl_4 (50.0 mg, 0.120 mmol) was dissolved in 3.00 mL of water and then filtered. Glacial acetic acid (4.00 mL) and dibenzo[*a,e*]cyclooctatetraene (24.5 mg, 0.120 mmol) were added, and the mixture was brought to reflux with stirring. Over 3 h the deep red solution slowly became yellow and a light yellow solid was deposited. The yellow solid was collected by filtration, washed with water, ethanol, and diethyl ether, and dried at 90 °C for 15 min. Yield: 46.0 mg (82%). Crystals for X-ray analysis were obtained by recrystallization from CD_2Cl_2/ether at −30 °C. Anal. Calcd (found) for $C_{16}H_{12}PtCl_2 \cdot {}^1/_2CH_2Cl_2$: C, 38.59 (38.97); H. 2.53 (2.33). ^{1}H NMR (250 MHz, CD_2Cl_2): 7.17 (s, 8H, aromatic CH), 6.56 (s with satellites, J_{Pt-H} = 59.3 Hz, 4H, olefinic CH). ^{195}Pt NMR (64.5 MHz, CD_2Cl_2): −2975 (quintet, J_{Pt-H} = 59.3 Hz). ^{13}C{^{1}H} NMR (300 MHz, CD_2Cl_2): 139.2 (s, aromatic), 129.0 (s, aromatic), 126.8 (s, aromatic), 98.0 (s with satellites, J_{Pt-C} = 136.3 Hz, olefinic C).

Dichloro(dibenzo[*a,e*]cyclooctatetraene)palladium(II), $PdCl_2$(DBCOT) (3). Na_2PdCl_4 (50.0 mg, 0.170 mmol) was dissolved in 4.00 mL of dry methanol and then filtered. The dark red filtrate was vigorously stirred with solid dichlorodibenzo[*a,e*]cyclooctatetraene (34.6 mg, 0.170 mmol). The color of the mixture change from red to yellow within 15 min. Stirring was continued for 4 h. Half of the solvent was removed in vacuo, and ether (8 mL) was added. The resulting microcrystalline yellow solid was isolated by filtration, washed with methanol and diethyl ether, and dried in vacuo. Yield: 52.3 mg (79%). Crystals for X-ray analysis were obtained by recrystallization from CD_2Cl_2/ether at −30 °C. Anal. Calcd (found) for $C_{16}H_{12}PdCl_2 \cdot$MeOH: C, 49.39 (49.41); H. 3.87 (3.48). ^{1}H NMR (250 MHz, CD_2Cl_2): 7.28−7.13 (m, 8H, aromatic CH), 6.95 (s, 4H, olefinic CH).

Diiodo(dibenzo[*a,e*]cyclooctatetraene)platinum(II), PtI_2(DBCOT) (4). Solid NaI (30.0 mg, 0.200 mmol) was added to a suspension of $PtCl_2$(DBCOT) (47.0 mg, 0.100 mmol) in acetone (4 mL). The solution immediately turned orange. The mixture was further stirred for 10 min and then concentrated in vacuo to ca. 2 mL. The resulting orange solid was collected by filtration and washed with water and diethyl ether. Yield: 64.0 mg (98%). Crystals for the X-ray analysis were obtained by recrystallization from CD_2Cl_2/ether at −30 °C. Anal. Calcd (found) for $C_{16}H_{12}PtI_2 \cdot {}^1/_2CH_2Cl_2$: C, 28.44 (28.72); H. 1.86 (1.90). ^{1}H NMR (250 MHz, CD_2Cl_2): 7.16 (s, 8H, aromatic CH), 6.87 (s with satellites, J_{Pt-H} = 59.0 Hz, 4H, olefinic CH). ^{195}Pt NMR (64.3 MHz, CD_2Cl_2): −2440 (quintet, J_{Pt-H} = 59.0 Hz).

Diphenyl(dibenzo[*a,e*]cyclooctatetraene)platinum(II), $PtPh_2$(DBCOT) (5). In a drybox a diethyl ether solution of phenylmagnesium bromide (3 M, 0.26 mmol) was added dropwise to a stirred solution of PtI_2(DBCOT) (73.00 mg, 0.112 mmol) in 6.00 mL of diethyl ether, and the reaction mixture was allowed to stir at room temperature for 12 h. The reaction mixture was brought outside the drybox and hydrolyzed with an ice-cold saturated aqueous solution of ammonium chloride. The ether layer was separated, and the water layer was extracted with two 20 mL portions of diethyl ether. The combined ether extracts were dried over anhydrous $MgSO_4$ containing a small amount of activated charcoal. The solution was filtered through diatomaceous earth, and the volatiles were removed in vacuo. The yellow solid residue was crystallized from a mixture of dichloromethane and ether. Yield: 50.0 mg (81%). Anal. Calcd (found) for $C_{28}H_{22}Pt \cdot 0.5CH_2Cl_2$: C, 57.38 (57.02); H. 3.85 (3.90). ^{1}H NMR (300 MHz, CD_2Cl_2): 7.63−7.04 (m, 30H, aromatic CH) 6.90−6.77 (m, 8H, aromatic CH), 6.14 (s with satellites, J_{Pt-H} = 33.0 Hz, 4H, olefinic CH). ^{195}Pt NMR (64.5 MHz, CD_2Cl_2): −3260 (s).

Table 5. Calculated Equilibrium Constants for Eq 8

	reactant ratio				
	1:0.5	1:1	1:1.5	1:3	
K	9.7	7.6	7.9	6.8	av = 8(1)

[Pt(μ^3-O)(DBCOT)(AuPPh$_3$)]$_3$(BF$_4$)$_3$ (6). A solution of $PtCl_2$(DBCOT) (94.0 mg, 0.200 mmol) in THF (50 mL) was vigorously stirred with solid $[(Ph_3PAu)_3(\mu^3\text{-O})]BF_4$ (296 mg. 0.200 mmol). The mixture became homogeneous and orange within 40 min. Stirring was continued for 2 h, and then the volume of the solution was reduced in vacuo to ca. 25 mL. Ether (50 mL) was added and the mixture cooled at −30 °C for 24 h. The resulting pale yellow-orange microcrystalline solid was isolated by filtration and dried in vacuo. Yield: 158 mg (82%). Crystals for X-ray analysis were obtained by recrystallization from $CDCl_3/CD_2Cl_2$. Anal. Calcd (found) for $C_{102}H_{81}Au_3B_3F_{12}O_3P_3Pt_3 \cdot {}^1/_2CHCl_3$: C, 41.77 (41.67); H. 2.76 (2.87). ^{1}H NMR (250 MHz, CD_2Cl_2): 7.50−7.35 (m, 45H, Ph), 7.17−7.06 (m, 24H, CH), 6.83−6.80 (m, 12H, CH). ^{31}P{^{1}H} NMR (101.2 MHz, CD_2Cl_2): 27.4 (s). ^{195}Pt NMR (64.5 MHz, CD_2Cl_2): −2420 (s). MS (ESI/APC-direct infusion, MeCN, *m/z*): 500.06 (100%, $[Ph_3PAuNCMe]^+$), 721.1 (65%, $[(Ph_3P)_2Au]^+$), 953.09 (20%, $[(Ph_3PAu)_2Cl]^+$), 1289.54 (10%, $[C_{50}H_{39}AuO_2PPt_2]^{2+}$), 874.26 (5%, $[C_{102}H_{81}Au_3O_3P_3Pt_3]^{3+}$- or $[C_{68}H_{54}Au_2O_2P_2Pt_2]^{2+}$).

Reaction of [Ir(μ-Cl)(COD)]$_2$ with DBCOT. Four 5 mm NMR tubes were prepared with $[Ir(\mu\text{-Cl})(COD)]_2$ (10.0 mg, 0.014 mmol) dissolved in 0.7 mL of $CDCl_3$. Solid DBCOT was added to each tube in a ratio ($[Ir(\mu\text{-Cl})(COD)]_2$:DBDOT) of 1:0.5, 1:1, 1:1.5, or 1:3. Each mixture changed from yellow to yellow-orange within 10 min. ^{1}H NMR spectra were recorded repeatedly over a 3 h period and did not change from the first spectrum. For the 1:3 reaction a small amount of precipitate appeared after 1 h. Only after a day did the others deposit a solid. The integration ratios from the NMR spectra taken 20 min after mixing were used to calculate equilibrium constants for eq 8 given in Table 5. A second set of two samples was prepared with less $[Ir(\mu\text{-Cl})(COD)]_2$: A solution of $[Ir(\mu\text{-Cl})(COD)]_2$ (2.0 mg, 0.0029 mmol) in CD_2Cl_2 (0.4 mL) was added to a solution of DBCOT (1.2 mg, 0.0059 mmol) in CD_2Cl_2 (0.3 mL). The mixture changed from orange to red within 5 min and stayed homogeneous for a least a week. The ^{1}H NMR did not change over this time period and gave the same equilibrium constant as the more concentrated samples.

^{1}H NMR (300 MHz, CD_2Cl_2) for $Ir_2(\mu\text{-Cl})_2$(COD)(DBCOT): 7.05 (m, 4H, DBCOT), 6.92 (m, 4H, DBCOT), 5.33 (s, 4H, olefinic DBCOT), 4.29 (s, 4H, olefinic COD), 2.14 (m, 4H, COD), 1.50 (m, 4H, COD).

Acknowledgment. Support from the Chemical Sciences, Geosciences and Biosciences Division, Office of Basic Energy Sciences, Office of Science, U.S. Department of Energy (DE-FG02-88ER13880), is gratefully acknowledged. Grants from the National Science Foundation (CHE-9531247, -922183526, -8908304) provided a portion of the funds for the purchase of the NMR equipment.

Supporting Information Available: Details of the crystal structure determinations and crystallographic information files (CIF). This material is available free of charge via the Internet at http://pubs.acs.org.

OM050713W